

De Novo Design and Facile Synthesis of 2D Covalent Organic Frameworks: A Two-in-One Strategy

Yusen Li,[†] Qing Chen,[§] Tiantian Xu,[†] Zhen Xie,[†] Jingjuan Liu,[‡] Xiang Yu,[‡] Shengqian Ma,^{||} Tianshi Qin,[§] and Long Chen^{*,†,||}

[†]Department of Chemistry, Institute of Molecular Plus, and Tianjin Key Laboratory of Molecular Optoelectronic Science, Tianjin University, Tianjin 300072, P. R. China

[‡]Analytical and Testing Center, Jinan University, Guangzhou 510632, P. R. China

[§]Institute of Advanced Materials (IAM), Nanjing Tech University (Nanjing Tech), Nanjing 210009, P. R. China

^{||}Department of Chemistry, University of South Florida, 4202 East Fowler Avenue, Tampa, Florida 33620, United States

Supporting Information

ABSTRACT: We herein develop a two-in-one molecular design strategy for facile synthesis of 2D imine based covalent organic frameworks (COFs). The integration of two different functional groups (i.e., formyl and amino groups) in one simple pyrene molecule affords a bifunctional building block: 1,6-bis(4-formylphenyl)-3,8-bis(4-aminophenyl)pyrene (BFBAPy). Highly crystalline and porous Py-COFs can be easily prepared by the self-condensation of BFBAPy in various solvents, such as CH₂Cl₂, CHCl₃, tetrahydrofuran, methanol, ethanol, acetonitrile, and dimethylacetamide, etc. The current work, to the best of our knowledge, is a rare case of COF synthesis that exhibits excellent solvent adaptability. Highly crystalline Py-COF thin films have been readily fabricated on various substrates and exhibit potential

applications in hole transporting layers for perovskite solar cells. Furthermore, the versatility of this two-in-one strategy was also verified by two additional examples. The current work dramatically reduces the difficulty of COF synthesis, and such two-in-one strategy is anticipated to be applicable for the synthesis of other COFs constructed by different building blocks and linkages.



INTRODUCTION

Covalent organic frameworks (COFs) are an emerging class of crystalline porous materials which feature fascinating regular structures and versatile functions.¹ Since the seminal work reported by Yaghi in 2005,^{1a} COFs have received increasing research interest because of their promising applications in gas sorption and separation,² catalysis,³ environmental remediation,⁴ sensing,⁵ drug delivery,⁶ energy storage,⁷ and conversion⁸ and so forth. Many synthetic efforts have been devoted to advance the development of COFs and great successes have been achieved such as metal triflate assisted COF synthesis,^{9a} *p*-toluene sulfonic acid monohydrate (PTSA·H₂O) assisted solid state synthesis,^{9b} and mechanochemical synthesis,^{9c} etc. However, most of the reported COFs are synthesized either by two-component or multiple-component¹⁰ co-condensation of at least two monomers bearing respectively different functional groups, with the exception of self-condensation of boronic acid (e.g., COF-1^{1a}) or aromatic nitriles (i.e., CTFs¹¹) (Scheme 1a). Furthermore, COFs are mostly prepared in delicately screened solvent mixtures and suffer from exhaustive trial-and-error procedures on selection and adjustment of the synthetic condition parameters like solvent combinations, temperature, reaction time, concen-

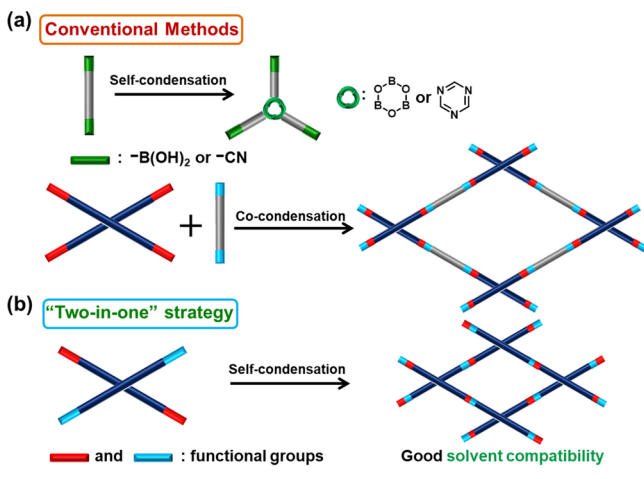
trations, pressure, etc.^{12a} Thus, a de novo molecular design strategy to simplify the synthesis of COFs in a more reliable and versatile way is highly desirable for advancing this research area.

We reason that one possible cause for the difficulties in preparing highly crystalline COFs lies in the deviation of the proper ratios among the dissolved comonomers due to the solubility difference. In most cases, the monomers are only partially dissolved during the solvothermal synthesis.^{12a} It is difficult to find a suitable solvent combination in which the monomers are soluble and maintain the stoichiometry to ensure sufficient 2D or 3D polymerization. To solve this dilemma, we envision that merging two different functional groups of the comonomers into a single molecule (i.e., “two-in-one” strategy) could bring several advantages: (i) the ideal stoichiometry could be perfectly maintained either in homogeneous or heterogeneous states during the polymerization process; (ii) the solvent adaptability could be greatly improved which could benefit the premodification of the substrate for COF films growth or postfabrication of the COF

Received: March 31, 2019

Published: August 13, 2019

Scheme 1. Diagrams for 2D COFs Constructed by (a) Conventional Self- and Co-condensation Methods and (b) Our New Two-in-One Strategy



films for device applications;¹³ last but not least (iii) the reproducibility of COF synthesis and their crystallinity could be greatly improved as well as the screening process of synthetic conditions could be simplified and become much easier.

For a proof-of-concept, herein we designed and synthesized a new bifunctional monomer 1,6-bis(4-formylphenyl)-3,8-bis(4-aminophenyl)pyrene (Figure 1a, BFBAPy) with two

formyl and two amino groups in a single pyrene core molecule to construct 2D pyrene-based imine COF (Py-COF) through intermolecular self-condensation. Unlike most reported COFs which involve the co-condensation of two or more kinds of monomers with separately different functional groups, this bifunctional module can be readily used for the construction of crystalline Py-COF in various solvents (Table S1 of the Supporting Information, SI). The stoichiometry of the two different functional groups was strictly guaranteed (1:1) in these systems, which is beneficial to the formation of regular structures. Actually, highly crystalline Py-COFs were obtained not only in mixed solvents (e.g., *o*-dichlorobenzene and *n*-butyl alcohol) but also in a series of mono organic solvent systems such as dichloromethane (DCM), chloroform, tetrahydrofuran (THF), methanol, ethanol, acetonitrile (MeCN), and dimethylacetamide (DMAc) and so forth. To the best of our knowledge, this is a rare case of COF synthesis that exhibits such excellent solvent adaptability. Besides, the reported Py-Py COF^{5c} which has similar structure with Py-COF was synthesized as a counterpart by the conventional co-condensation approach. By comparison of the PXRD patterns and surface areas, it clearly indicates that Py-COF exhibits higher crystallinity than Py-Py COF (Figure S34). Furthermore, the Py-Py COF constructed by co-condensation method exhibits poor solvent adaptability with largely solvent dependent crystallinity. (Figure S34b). Moreover, this two-in-one design strategy also facilitates successful growth of high quality Py-COF thin films on various substrates like transparent glass, conducting indium tin oxide (ITO), and silicon wafer with

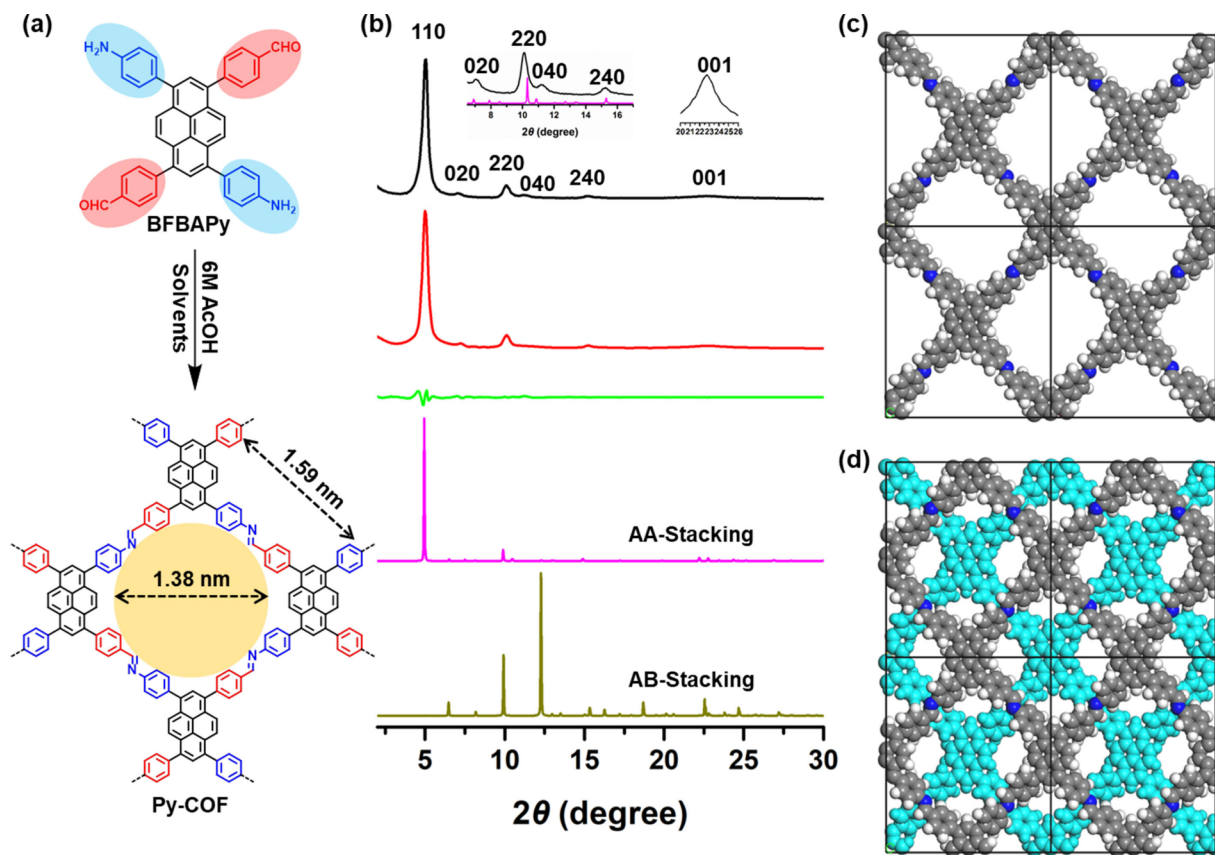


Figure 1. (a) The synthesis of Py-COF using single bifunctional monomer BFBAPy; (b) experimental PXRD patterns of Py-COF_{DCM} (black), Pawley refinement (red), their difference (green), simulated profiles using AA-stacking (purple), and AB-stacking (dark yellow) modes; (c) unit cells of AA-stacking; and (d) AB-stacking mode.

good crystallinity. In addition, two new COFs (BFBAEB-COF and BFBAEPy-COF) with dual-pore structures, which cannot be constructed by a dual monomer approach (Schemes S9 and S10), had been successfully synthesized to verify the versatility of this two-in-one strategy.

RESULTS AND DISCUSSION

Synthesis and Characterization. As shown in Scheme S1, BFBAPy was prepared via a facile three-step route in high yield and unambiguously characterized by NMR, MALDI-TOF MS and single crystal X-ray diffraction analysis (Figure S16). In a typical synthetic procedure of Py-COFs (Figure S22), BFBAPy (29.6 mg, 0.05 mmol) was suspended in a mixture of organic solvent (2 mL) and 6 M acetic acid (0.2 mL) followed by refluxing for 72 h to afford orange crystalline solids (denoted as Py-COF_{solvent}) in high yields. Fourier transform infrared (FT-IR) spectra of Py-COF_{DCM} and the monomer BFBAPy were compared in Figure S1. The disappearance of N–H (~ 3470 and 3360 cm^{-1}) vibration, dramatic attenuation of C=O (1680 cm^{-1}) stretching bands and the appearance of new intensive imine (C=N) band at 1628 cm^{-1} confirmed the high polycondensation degree of Py-COF.¹⁴ All the IR spectra of Py-COFs synthesized from different solvents are nearly identical (Figure S1b). The formation of imine linkages was further verified by ¹³C solid-state NMR spectroscopy, with an obvious characteristic peak at 156 ppm assignable to the carbon of C=N double bonds.¹⁴ Other aromatic carbon signals can be properly assigned as well (Figure S2). Elemental analysis indicated that the C, H, and N contents of the COFs were in good agreement with the theoretical values expected for an infinite 2D sheet.

Interestingly, Py-COFs prepared from varied solvents exhibited significantly different morphologies as revealed by the scanning electron microscopies (Figure S6). For example, spherical, rodlike, and platelike aggregates composed of small nanoparticles (Figure S6c, d) or nanoflakes (Figure S6a, e, h) were observed. These differences were probably caused by the solvent polarity variation as reported before.^{16a} Transmission electron microscopy proved a nearly uniform porous texture (Figure S7).

Crystalline Structure. The crystallinity of Py-COFs synthesized from different solvents was examined by powder X-ray diffraction (PXRD) measurements. Actually, all the Py-COFs exhibited strong diffraction peaks at 5.02° , 7.04° , 10.18° , 11.19° , 15.28° , and 22.75° (Figure S4), which could be indexed to (110), (020), (220), (040), (240), and (001) facets, respectively. The first dominant diffraction peak at 5.02° corresponded to the *d*-spacing of 1.70 nm, which was in good agreement with the calculated length of the tetragon (1.59 nm, Figure 1a). The PXRD pattern of Py-COF_{DCM} was selected as the representative experimental data to simulate the lattice packing model. As shown in Figure 1b, the calculated PXRD pattern of AA stacking model (purple) was in accordance with the experimental ones (black), whereas the staggered AB stacking pattern (dark yellow) exhibits significant difference from the experimental PXRD data. Furthermore, the profile of Pawley refinement matched well with the observed signals as evident by their negligible deviation (green) (Figure 1b) with the final R_{wp} and R_p values converged to 5.57% and 4.16%, respectively. The Pawley refinement afforded a *P21* monoclinic space group with unit cell parameters of $a = 24.3740$ Å, $b = 26.2134$ Å, $c = 4.0287$ Å, $\alpha = \gamma = 90^\circ$, and $\beta = 72.1^\circ$.

Porosity of Py-COFs. The permanent porosity of Py-COFs was assessed by N₂ sorption measurements at 77 K (Figure 2a). All the Py-COFs displayed reversible type I isotherms with

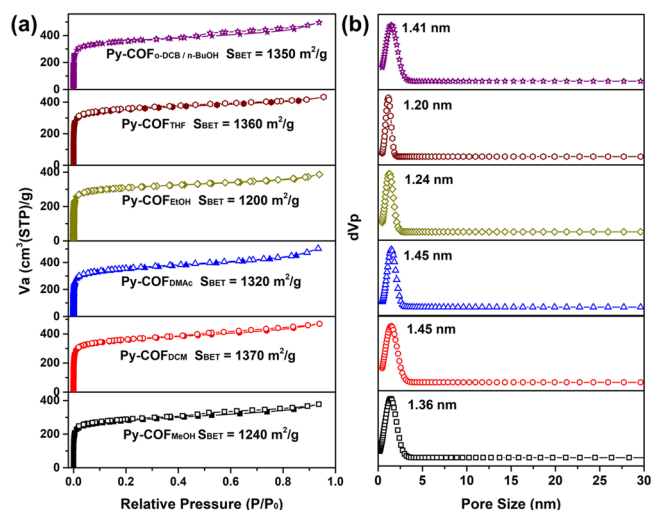


Figure 2. (a) Nitrogen adsorption (solid) and desorption (open) isotherms at 77 K and (b) pore size distribution curves based on NLDFT calculation for Py-COF_{MeOH} (black), Py-COF_{DCM} (red), Py-COF_{DMAC} (blue), Py-COF_{EtOH} (dark yellow), Py-COF_{THF} (wine), and Py-COF_{6-DCB/n-BuOH} (purple).

rapid N₂ uptakes at the low relative pressure range $P/P_0 < 0.05$, characteristic of microporous materials.¹⁵ Brunauer–Emmett–Teller (BET) surface areas calculated from the N₂ adsorption isotherms in the low pressure region revealed that all the Py-COFs exhibited high specific surface areas (1200–1370 m^2/g , Figure S17) which are close to the theoretical value (1537 m^2/g) calculated by High-Throughput-based Complex Adsorption and Diffusion Simulation Suite (HT-CADSS) according to the literature method.^{15c} The pore size distribution analysis of Py-COFs based on the nonlocal density functional theory (NLDFT) indicated one main distribution centered at the range of 1.20–1.45 nm (Figure 2b), which is close to the theoretical value (1.38 nm, Figure 1a).

Stability of Py-COFs. The chemical stability of Py-COF_{DCM} was further examined by keeping the samples under boiling water, aqueous NaOH (12 M) and HCl (12 M) solutions for 3 days. All the samples retained their crystallinity, porosity, and chemical constitution upon treatments in these harsh conditions. For example, after the treatments, the PXRD patterns (Figure S9a), surface areas (Figure S9b) and FT-IR spectra (Figure S10) remained unchanged. Interestingly, crystalline Py-COF can also be obtained in 6 M AcOH and 12 M HCl without adding any organic solvents (denoted as Py-COF_{6M AcOH} and Py-COF_{12M HCl}, Figure S24), which indicates Py-COF can also be formed and survived in those harsh conditions. These control experiments reasonably corroborate the extraordinary chemical stability of Py-COF in strong acidic condition. Furthermore, the high hydrophobicity (Figure S23) might also contribute to the high stability of Py-COF_{DCM} toward strong acid and base, which protecting Py-COF_{DCM} from hydrolysis^{16b} and remains their high crystallinity (Figure S4). However, the thermogravimetric analysis (TGA) result indicated that Py-COF_{DCM} was thermally stable up to 400 °C, and displayed only 25% weight loss even heated at 800 °C

(Figure S3). Such superior stabilities render Py-COFs to be good candidates for potential applications in catalysis,³ environmental remediation,⁴ and energy storage related areas.⁷

Monitoring of Py-COF Formation Process. To shed more insights into the growth of Py-COFs, time-dependent condensations were conducted in CH_2Cl_2 for monitoring the evolution of the porous crystalline network. The condensation reactions were thus carried out at 0.5, 1, 2, 5, 9, 15, and 24 h. PXRD measurements were utilized to monitor their crystallinity. As shown in Figure 3a, the characteristic peak ($2\theta =$

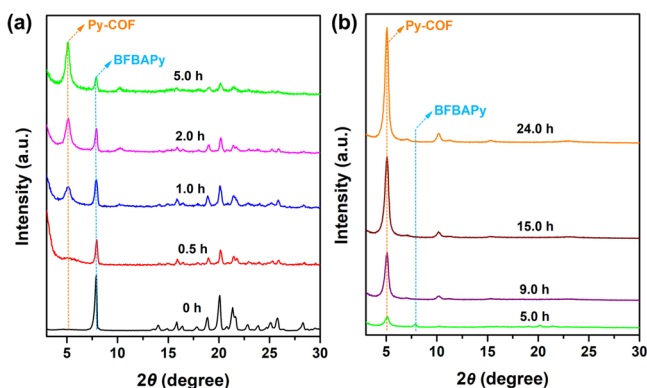


Figure 3. PXRD patterns of Py-COF_{DCM} at different reaction times: (a) 0–5 h; (b) 5–24 h.

5.02°) for Py-COFs became visible after 0.5 h and increased to be distinctive at ca. 1 h. With further elongation of reaction time, the characteristic peak of Py-COF became dominant while the diffraction peak for the monomer BFBAPy ($2\theta = 7.90^\circ$) exhibited dramatic attenuations (0–5 h) and completely disappeared after ca. 9 h (Figure 3b). A highly crystalline Py-COF sample can be obtained after 24 h (Figure 3b) and the intensity of diffraction peak did not exhibit further enhancement after 36 h (Figure S14). Unlike the rapid formation of crystalline boronate ester COFs at the nucleation stage (within minutes),¹² the growth of Py-COFs were consistent with most reported imine-based COFs, which involved an initial rapid precipitation of amorphous polymer network (ca. 0–0.5 h) followed by gradual amorphous-to-crystalline transformation step (0.5–24 h).¹⁷ Furthermore, highly crystalline Py-COFs can be synthesized under different atmospheres and at relative low concentrations (Figures S11–S13), which greatly simplified the synthetic procedure.

Meanwhile, the impact of stoichiometric imbalance on Py-COF was also explored.^{17d} The intensity of Py-COF exhibited obvious decrement while the full width at half-maximum (fwhm) of the (100) diffraction peak at 5.02° showcased gradual increase when different amounts (5%, 10%, 25%, and 50%) of 1,3,6,8-tetrakis(4-aminophenyl)pyrene ($\text{Py}(\text{NH}_2)_4$) were added in Py-COF_{DCM} reaction system. The surface areas of these controlled samples also exhibited distinct decrease (Figure S33c). These results jointly indicated that the more $\text{Py}(\text{NH}_2)_4$ was added, the worse the crystallinity became (Figure S33a). The similar tendency was observed when different amounts of aniline modulator¹⁴ were added to the reaction system (Figures S33b, d). These observations are different from the previous reported examples using co-condensation strategy where the addition of modulator and the stoichiometric imbalance did greatly improved the crystallinity of the resultant COFs.^{10f,17d,18} Thus, in our current cases, the

stoichiometric imbalance might be insensitive to the crystallinity of the COFs because both functional moieties either are or are not soluble in different reaction conditions, and it became easier to find suitable conditions that work for COFs formation in this “two-in-one” systems that leads to the good solvent adaptability.

Growth and Characterization of Py-COF Films. COFs are usually obtained as insoluble powders, which hamper their practical applications to some extent, especially for electronic devices. Recently, oriented COF thin films have been developed and served as active materials in optoelectronic devices¹⁹ and photoelectrodes for water splitting.²⁰ These studies prompted us to grow Py-COF thin films using our bifunctional monomer BFBAPy on various substrates such as glass, ITO substrate, and silicon wafer. The successful growth of highly crystalline Py-COF films on these substrates was proven by their appearance of strong diffraction peaks at 5.02° as that of Py-COF powder (Figure 4a). UV–vis absorption

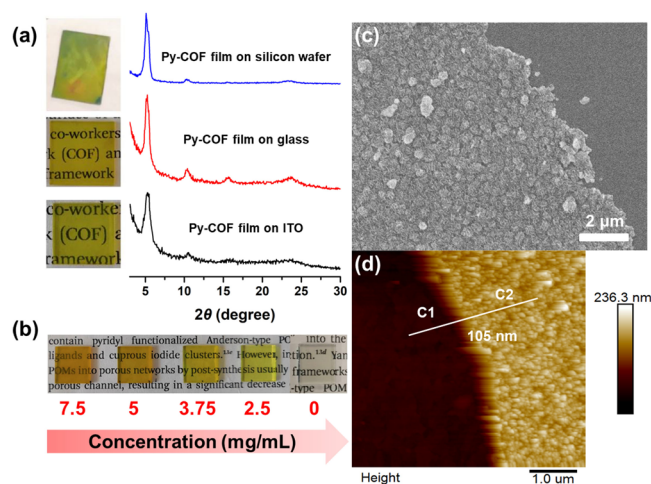


Figure 4. (a) Photograph and grazing incidence XRD (GI-XRD) patterns of Py-COF films grown on different substrates (3.75 mg/mL) with an incidence angle of 0.2°. (b) Optical images of Py-COF films obtained in varied monomer concentrations on glass. (c) SEM image of Py-COF film grown on glass; (d) AFM images of Py-COF thin film (3.75 mg/mL).

spectra of Py-COF film and powder were compared with that of the monomer in Figure S8. Both of them exhibited intensive light absorption in the visible light region. The absorption onset of Py-COF powder and film were 552 and 557 nm, which displayed a slight red shift compared with that of BFBAPy (544 nm). SEM images of the transparent Py-COF film on glass indicated the thin films were continuous and composed of evenly distributed crystalline particles up to ca. 500 nm in size (Figure 4c). AFM images of the Py-COF thin film (3.75 mg/mL) revealed a thickness of 105 nm (Figure 4d) with root-mean-square (RMS) roughness of 10.14 nm (Figure S19). The orientation of Py-COF film was investigated by 2D synchrotron radiation grazing incidence wide-angle X-ray scattering (2D-GIWAXS). The ring-like scattering pattern indicated Py-COF film exhibited almost no preferred orientation (Figure S32). The film thickness could be readily tuned (Figure S18) by controlling the “initial concentration” of the monomer, which can be recognized by the naked eye (Figure 4b). Compared with other reported COF films,^{19,20} the current Py-COF films exhibit better substrate adaptability

(Figure 4a), less solvent dependence (Figure S20) and better transparency (Figure S21). And such solvent adaptability for Py-COF synthesis make it possible to grow high quality film on ITO substrate with PEDOT/PSS coating (Figure S26). These features would greatly facilitate their potential applications in optoelectronics.²¹ For example, a preliminary trial of such film applied as the hole transporting layers in perovskite solar cell²² was demonstrated. As shown in Figure 5, the device based on

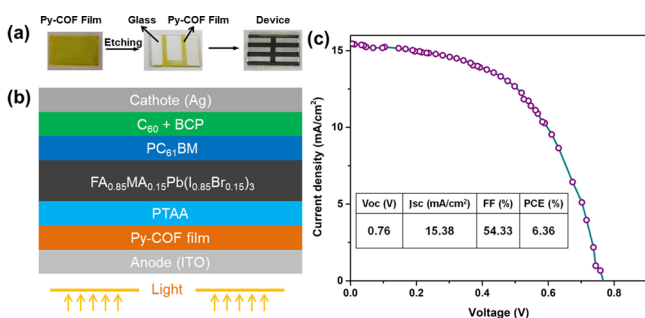


Figure 5. (a) The schematic illustration of the device (with an exposed active area of 0.03 cm²) fabrication process; (b) the device architecture; and (c) current density–voltage (J – V) characteristic curve under AM 1.5G 100 mW cm⁻² simulated solar light by utilizing Py-COF film as the hole transporting layer in perovskite solar cell.

the mixed perovskite (FA_{0.85}MA_{0.15}Pb(I_{0.85}Br_{0.15})₃)^{22b} that comprising formamidinium lead iodide (FAPbI₃, 85%) and methylammonium lead bromide (MAPbBr₃, 15%) showed an open-circuit voltage (V_{oc}) of 0.76 V, a short-circuit current (J_{sc}) of 15.38 mA/cm², and a filled factor (FF) of 54.33%, which resulted in a power conversion efficiency (PCE) of 6.36%.^{22c} The performance of the resulting device is moderate (Table S6); this experiment is a proof-of-concept demonstration of using transparent COF thin films for optoelectronics. Improved photoenergy conversion efficiency would be achievable when more matched energy gaps, better interfacial quality, and large-area-oriented COFs films with less grain boundaries are available.

Versatility of the Two-in-One Strategy. In order to illustrate the generality and tolerance of the two-in-one strategy, another two bifunctional monomers, 1,4-bis(4-formylphenyl)-2,5-bis((4-aminophenyl)ethynyl) benzene (BFBAEB) and 1,6-bis(4-formylphenyl)-3,8-bis((4-aminophenyl)ethynyl)pyrene (BFBAEPy) (Figure 6a), were designed and synthesized to construct two new COFs. As expected, two corresponding crystalline COFs were facilely synthesized in at least three different simplex organic solvents (Figure S27). The PXRD pattern of BFBAEB-COF displays strong diffraction at 2.95°, 5.94°, 8.93°, 11.95°, 14.97°, and 24.07°, which could be assigned to (100), (200), (300), (400), (500), and (001) facets. Similarly, the diffraction peaks for BFBAEPy-COF appear at 2.54°, 4.55°, 5.30°, 6.97°, 9.29°, and 24.00°, which were ascribed to the (100), (110), (200), (210), (310), and (001) diffractions. It is noteworthy that both the experimental PXRD results coincide well with the simulated hexagonal AA-stacking models (Figures 6b, c), which is different from the Py-COF (orthorhombic structure). The details of structural simulation are summarized in Figures S28 and S29 and Tables S4–S5. The chemical constitution and porosity of the two COFs were further confirmed by FI-IR and N₂ sorption isotherms (Figures S30 and S31). Interestingly, these two COFs built from the bifunctional monomers

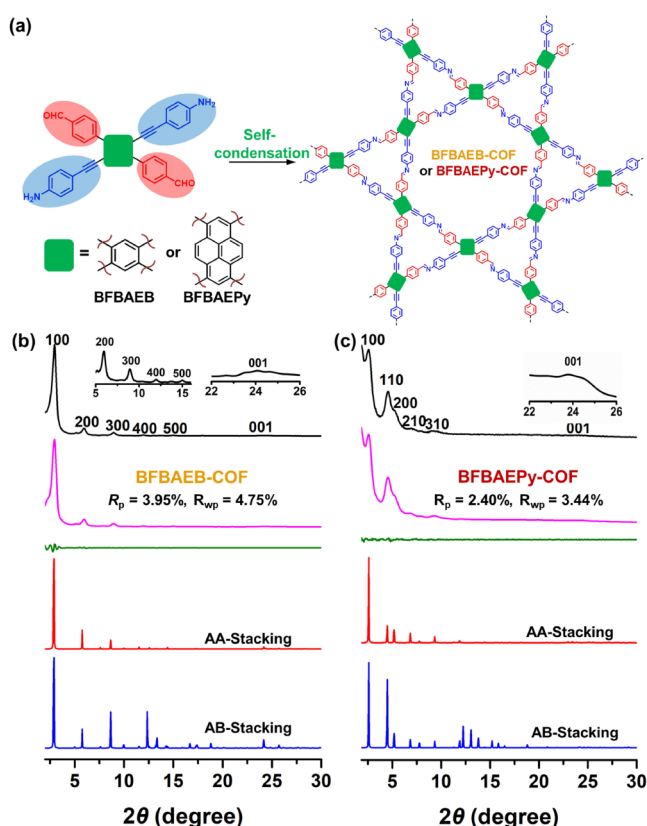


Figure 6. (a) Self-condensation of two new bifunctional monomers BFBAEB and BFBAEPy to obtain the corresponding COFs. Experimental PXRD patterns (black), Pawley refinement (purple), their difference (green), simulated profiles using AA-stacking (red), and AB-stacking (blue) modes for (b) BFBAEB-COF and (c) BFBAEPy-COF.

(BFBAEB and BFBAEPy) with different substituted arm length preferred to form heteroporous COFs with dual pores, which were demonstrated by both the PXRD results and the pore size distribution analysis (Figure S31). It is noteworthy that these two dual-pore COFs with Kagome structures cannot be formed by co-condensation of corresponding building blocks (Schemes S9 and S10) which were also demonstrated by the control experiments. For example, the co-condensation of TEAB and TFPB failed to give any crystalline COF upon 10 different conditions screening (Figure S35). However, the co-condensation of TAEpy and Py(CHO)₄ afforded TAEpy-COF only in specific solvent combinations (Figure S36) but resulted in a single pore rhombic structure (Figure S37). These results further confirm the rationality and feasibility of our two-in-one molecular design strategy for new COF synthesis.

CONCLUSIONS

In summary, we successfully developed a two-in-one molecular design strategy to construct 2D imine COFs in easy and versatile conditions. The use of single organic solvent as the reaction media greatly facilitates the preparation of COFs. Furthermore, it is readily possible to grow continuous Py-COF thin films in high quality on various substrates based on the “two-in-one” monomer. This strategy is also demonstrated to be applicable for other two COFs synthesis with different building blocks. Moreover, it could also be extended to different synthetic techniques like chemical vapor deposition^{23a} and interface-assisted synthesis^{23b} of molecular frameworks.

Although more synthetic efforts are needed for obtaining the elaborately designed bifunctional monomers, it is worthwhile to consider the merits mentioned above. The utilization of the “two-in-one” approach to construct crystalline COFs based on a series of new building blocks and/or new linkages is currently ongoing in our laboratory.

■ ASSOCIATED CONTENT

● Supporting Information

The Supporting Information is available free of charge on the ACS Publications website at DOI: 10.1021/jacs.9b03463.

Experiment details and characterization of the monomer and Py-COFs (PDF)

Crystallographic data (CIF)

■ AUTHOR INFORMATION

Corresponding Author

*long.chen@tju.edu.cn

ORCID

Shengqian Ma: 0000-0002-1897-7069

Long Chen: 0000-0001-5908-266X

Notes

The authors declare no competing financial interest.

■ ACKNOWLEDGMENTS

This work was financially supported by the National Key Research and Development Program of China (2017YFA0207500) and the Natural Science Foundation of Tianjin (17JCJQC44600). We thank Prof. Dong Wang at Institute of Chemistry, Chinese Academy of Sciences for his kind help on the measurement of 2D-GIWAXS.

■ REFERENCES

- (1) (a) Coté, A. P.; Benin, A. I.; Ockwig, N. W.; O’Keeffe, M.; Matzger, A. J.; Yaghi, O. M. Porous, Crystalline, Covalent Organic Frameworks. *Science* **2005**, *310*, 1166–1170. (b) Diercks, C. S.; Yaghi, O. M. The atom, the molecule, and the Covalent Organic Framework. *Science* **2017**, *355*, 923. (c) Huang, N.; Wang, P.; Jiang, D. Covalent Organic Frameworks: A Materials Platform for Structural and Functional Designs. *Nat. Rev. Mater.* **2016**, *1*, 16068. (d) Song, Y.; Sun, Q.; Aguila, B.; Ma, S. Opportunities of Covalent Organic Frameworks for Advanced Applications. *Adv. Sci.* **2019**, *6*, 1801410. (e) Auras, F.; Ascherl, L.; Hakimioun, A. H.; Margraf, J. T.; Hanusch, F. C.; Reuter, S.; Bessinger, D.; Doblinger, M.; Hettstedt, C.; Karaghiosoff, K.; et al. Synchronized Offset Stacking: A Concept for Growing Large-Domain and Highly Crystalline 2D Covalent Organic Frameworks. *J. Am. Chem. Soc.* **2016**, *138*, 16703–16710. (f) Ascherl, L.; Sick, T.; Margraf, J. T.; Lapidus, S. H.; Calik, M.; Hettstedt, C.; Karaghiosoff, K.; Doblinger, M.; Clark, T.; Chapman, K. W.; Auras, F.; Bein, T. Molecular Docking Sites Designed for the Generation of Highly Crystalline Covalent Organic Frameworks. *Nat. Chem.* **2016**, *8*, 310–316.
- (2) (a) Huang, N.; Krishna, R.; Jiang, D. Tailor-Made Pore Surface Engineering in Covalent Organic Frameworks: Systematic Functionalization for Performance Screening. *J. Am. Chem. Soc.* **2015**, *137*, 7079–7082. (b) Furukawa, H.; Yaghi, O. M. Storage of Hydrogen, Methane, and Carbon Dioxide in Highly Porous Covalent Organic Frameworks for Clean Energy Applications. *J. Am. Chem. Soc.* **2009**, *131*, 8875–8883. (c) Zeng, Y.; Zou, R.; Zhao, Y. Covalent Organic Frameworks for CO₂ Capture. *Adv. Mater.* **2016**, *28*, 2855–2873.

(d) Fan, H.; Mundstock, A.; Feldhoff, A.; Knebel, A.; Gu, J.; Meng, H.; Caro, J. Covalent Organic Framework-Covalent Organic Framework Bilayer Membranes for Highly Selective Gas Separation. *J. Am. Chem. Soc.* **2018**, *140*, 10094–10098.

(3) (a) Ding, S.-Y.; Gao, J.; Wang, Q.; Zhang, Y.; Song, W.-G.; Su, C.-Y.; Wang, W. Construction of Covalent Organic Framework for Catalysis: Pd/COF-LZU1 in Suzuki-Miyaura Coupling Reaction. *J. Am. Chem. Soc.* **2011**, *133*, 19816–19822. (b) Lin, S.; Diercks, C. S.; Zhang, Y.-B.; Kornienko, N.; Nichols, E. M.; Zhao, Y.; Paris, A. R.; Kim, D.; Yang, P.; Yaghi, O. M.; Chang, C. J. Covalent Organic Frameworks Comprising Cobalt Porphyrins for Catalytic CO₂ Reduction in Water. *Scienc* **2015**, *349*, 1208–1213. (c) Sun, Q.; Aguila, B.; Perman, J. A.; Nguyen, N. T.-K.; Ma, S. Flexibility Matters: Cooperative Active Sites in Covalent Organic Framework and Threaded Ionic Polymer. *J. Am. Chem. Soc.* **2016**, *138*, 15790–15796.

(4) (a) Sun, Q.; Aguila, B.; Earl, L. D.; Abney, C. W.; Wojtas, L.; Thallapally, P. K.; Ma, S. Covalent Organic Frameworks as a Decorating Platform for Utilization and Affinity Enhancement of Chelating Sites for Radionuclide Sequestration. *Adv. Mater.* **2018**, *30*, 1705479. (b) Ji, W.; Xiao, L.; Ling, Y.; Ching, C.; Matsumoto, M.; Bisbey, R. P.; Helbling, D. E.; Dichtel, W. R. Removal of GenX and Perfluorinated Alkyl Substances from Water by Amine-Functionalized Covalent Organic Frameworks. *J. Am. Chem. Soc.* **2018**, *140*, 12677–12681.

(5) (a) Lin, G.; Ding, H.; Yuan, D.; Wang, B.; Wang, C. A Pyrene-Based, Fluorescent Three-Dimensional Covalent Organic Framework. *J. Am. Chem. Soc.* **2016**, *138*, 3302–3305. (b) Hao, Q.; Zhao, C.; Sun, B.; Lu, C.; Liu, J.; Liu, M.; Wan, L.-J.; Wang, D. Confined Synthesis of Two-Dimensional Covalent Organic Framework Thin Films within Superspreading Water Layer. *J. Am. Chem. Soc.* **2018**, *140*, 12152–12158. (c) Ascherl, L.; Evans, E. W.; Hennemann, M.; Di Nuzzo, D.; Hufnagel, A. G.; Beetz, M.; Friend, R. H.; Clark, T.; Bein, T.; Auras, F. Solvatochromic Covalent Organic Frameworks. *Nat. Commun.* **2018**, *9*, 3802.

(6) (a) Mitra, S.; Sasmal, H. S.; Kundu, T.; Kandambeth, S.; Illath, K.; Díaz Díaz, D.; Banerjee, R. Targeted Drug Delivery in Covalent Organic Nanosheets (CONs) via Sequential Postsynthetic Modification. *J. Am. Chem. Soc.* **2017**, *139*, 4513–4520. (b) Zhang, G.; Li, X.; Liao, Q.; Liu, Y.; Xi, K.; Huang, W.; Jia, X. Water-Dispersible PEG-Curcumin/Amine-Functionalized Covalent Organic Framework Nanocomposites as Smart Carriers for in Vivo Drug Delivery. *Nat. Commun.* **2018**, *9*, 2785.

(7) (a) DeBlase, C. R.; Silberstein, K. E.; Truong, T.-T.; Abruña, H. D.; Dichtel, W. R. β -Ketoenamine-Linked Covalent Organic Frameworks Capable of Pseudocapacitive Energy Storage. *J. Am. Chem. Soc.* **2013**, *135*, 16821–16824. (b) Halder, A.; Ghosh, M.; Khayum, M. A.; Bera, S.; Addicoat, M.; Sasmal, H. S.; Karak, S.; Kurungot, S.; Banerjee, R. Interlayer Hydrogen-Bonded Covalent Organic Frameworks as High-Performance Supercapacitors. *J. Am. Chem. Soc.* **2018**, *140*, 10941–10945. (c) DeBlase, C. R.; Hernández-Burgos, K.; Silberstein, K. E.; Rodríguez-Calero, G. G.; Bisbey, R. P.; Abruña, H. D.; Dichtel, W. R. Rapid and Efficient Redox Processes within 2D Covalent Organic Framework Thin Films. *ACS Nano* **2015**, *9*, 3178–3183. (d) Vazquez-Molina, D. A.; Mohammad-Pour, G. S.; Lee, C.; Logan, M. W.; Duan, X.; Harper, J. K.; Uribe-Romo, F. J. Mechanically Shaped Two-dimensional Covalent Organic Frameworks Reveal Crystallographic Alignment and Fast Li-Ion Conductivity. *J. Am. Chem. Soc.* **2016**, *138*, 9767–9770.

(8) (a) Calik, M.; Auras, F.; Salonen, L. M.; Bader, K.; Grill, I.; Handloser, M.; Medina, D. D.; Dogru, M.; Löbermann, F.; Trauner, D.; Hartschuh, A.; Bein, T. Extraction of Photogenerated Electrons and Holes from a Covalent Organic Framework Integrated Heterojunction. *J. Am. Chem. Soc.* **2014**, *136*, 17802–17807. (b) Lin, C.-Y.; Zhang, D.; Zhao, Z.; Xia, Z. Covalent Organic Framework Electrocatalysts for Clean Energy Conversion. *Adv. Mater.* **2018**, *30*, 1703646.

(9) (a) Matsumoto, M.; Dasari, R. R.; Ji, W.; Feriante, C. H.; Parker, S.; Marder, T. C.; Dichtel, W. R. Rapid, Low Temperature Formation of Imine-Linked Covalent Organic Frameworks Catalyzed by Metal

- Triflates. *J. Am. Chem. Soc.* **2017**, *139*, 4999–5002. (b) Karak, S.; Kumar, S.; Pachfule, P.; Banerjee, R. Porosity Prediction through Hydrogen Bonding in Covalent Organic Frameworks. *J. Am. Chem. Soc.* **2018**, *140*, 5138–5145. (c) Biswal, B. P.; Chandra, S.; Kandambeth, S.; Lukose, B.; Heine, T.; Banerjee, R. Mechanochemical Synthesis of Chemically Stable Isoreticular Covalent Organic Frameworks. *J. Am. Chem. Soc.* **2013**, *135*, 5328–5331.
- (10) (a) Huang, N.; Zhai, L.; Coupny, D. E.; Addicoat, M. A.; Okushita, K.; Nishimura, K.; Heine, T.; Jiang, D. Multiple-Component Covalent Organic Frameworks. *Nat. Commun.* **2016**, *7*, 12325. (b) Liang, R.-R.; Xu, S.-Q.; Pang, Z.-F.; Qi, Q.-Y.; Zhao, X. Self-Sorted Pore-Formation in the Construction of Heteropore Covalent Organic Frameworks Based on Orthogonal Reactions. *Chem. Commun.* **2018**, *54*, 880–883. (c) Pang, Z.-F.; Xu, S.-Q.; Zhou, T.-Y.; Liang, R.-R.; Zhan, T.-G.; Zhao, X. Construction of Covalent Organic Frameworks Bearing Three Different Kinds of Pores through the Heterostructural Mixed Linker Strategy. *J. Am. Chem. Soc.* **2016**, *138*, 4710–4713. (d) Zeng, Y.; Zou, R.; Luo, Z.; Zhang, H.; Yao, X.; Ma, X.; Zou, R.; Zhao, Y. Covalent Organic Frameworks Formed with Two Types of Covalent Bonds Based on Orthogonal Reactions. *J. Am. Chem. Soc.* **2015**, *137*, 1020–1023. (e) Jin, Y.; Hu, Y.; Zhang, W. Tessellated Multiporous Two-dimensional Covalent Organic Frameworks. *Nat. Rev. Chem.* **2017**, *1*, 0056. (f) Waller, P. J.; Lyle, S. J.; Osborn Popp, T. M.; Diercks, C. S.; Reimer, J. A.; Yaghi, O. M. Chemical Conversion of Linkages in Covalent Organic Frameworks. *J. Am. Chem. Soc.* **2016**, *138*, 15519–15522.
- (11) Kuhn, P.; Antonietti, M.; Thomas, A. Porous, Covalent Triazine-Based Frameworks Prepared by Ionothermal Synthesis. *Angew. Chem., Int. Ed.* **2008**, *47*, 3450–3453.
- (12) (a) Smith, B. J.; Dichtel, W. R. Mechanistic Studies of Two-Dimensional Covalent Organic Frameworks Rapidly Polymerized from Initially Homogenous Conditions. *J. Am. Chem. Soc.* **2014**, *136*, 8783–8789. (b) Smith, B. J.; Hwang, N.; Chavez, A. D.; Novotney, J. L.; Dichtel, W. R. Growth Rates and Water Stability of 2D Boronate Ester Covalent Organic Frameworks. *Chem. Commun.* **2015**, *51*, 7532–7535.
- (13) Sun, Q.; Aguila, B.; Perman, J.; Butts, T.; Xiao, F.-S.; Ma, S. Integrating Superwettability within Covalent Organic Frameworks for Functional Coating. *Chem.* **2018**, *4*, 1726–1739.
- (14) Uribe-Romo, F. J.; Hunt, J. R.; Furukawa, H.; Klöck, O'Keeffe, M.; Yaghi, O. M. A Crystalline Imine-Linked 3-D Porous Covalent Organic Framework. *J. Am. Chem. Soc.* **2009**, *131*, 4570–4571.
- (15) (a) Weber, J.; Antonietti, M.; Thomas, A. Microporous Networks of High-Performance Polymers: Elastic Deformations and Gas Sorption Properties. *Macromolecules* **2008**, *41*, 2880–2885. (b) Thommes, M.; Kaneko, K.; Neimark, A. V.; Olivier, J. P.; Rodriguez-Reinoso, F.; Rouquerol, J.; Sing, K. S. W. Physisorption of Gases, with Special Reference to the Evaluation of Surface Area and Pore Size Distribution. *Pure Appl. Chem.* **2015**, *87*, 1051–1069. (c) Yang, Q.; Liu, D.; Zhong, C.; Li, J.-R. Development of Computational Methodologies for Metal-Organic Frameworks and Their Application in Gas Separations. *Chem. Rev.* **2013**, *113*, 8261–8323.
- (16) (a) Das, G.; Skorjanc, T.; Sharma, S. K.; Gandara, F.; Lusi, M.; Shankar Rao, D. S.; Vimala, S.; Krishna Prasad, S.; Raya, J.; Han, D. S.; et al. Viologen-Based Conjugated Covalent Organic Networks via Zincke Reaction. *J. Am. Chem. Soc.* **2017**, *139*, 9558–9565. (b) Kandambeth, S.; Mallick, A.; Lukose, B.; Mane, M. V.; Heine, T.; Banerjee, R. Construction of Crystalline 2D Covalent Organic Frameworks with Remarkable Chemical (Acid/Base) Stability via a Combined Reversible and Irreversible Route. *J. Am. Chem. Soc.* **2012**, *134*, 19524–19527.
- (17) (a) Smith, B. J.; Overholts, A. C.; Hwang, N.; Dichtel, W. R. Insight into The Crystallization of Amorphous Imine-Linked Polymer Networks to 2D Covalent Organic Frameworks. *Chem. Commun.* **2016**, *52*, 3690–3693. (b) Gao, Q.; Bai, L.; Zeng, Y.; Wang, P.; Zhang, X.; Zou, R.; Zhao, Y. Reconstruction of Covalent Organic Frameworks by Dynamic Equilibrium. *Chem. - Eur. J.* **2015**, *21*, 16818–16822. (c) Yuan, Y.-C.; Sun, B.; Cao, A.-M.; Wang, D.; Wan, L.-J. Heterogeneous Nucleation and Growth of Highly Crystalline Imine-Linked Covalent Organic Frameworks. *Chem. Commun.* **2018**, *54*, 5976–5979. (d) Calik, M.; Sick, T.; Dogru, M.; Döblinger, M.; Datz, S.; Budde, H.; Hartschuh, A.; Auras, F.; Bein, T. From Highly Crystalline to Outer Surface-Functionalized Covalent Organic Frameworks: A Modulation Approach. *J. Am. Chem. Soc.* **2016**, *138*, 1234–1239.
- (18) Ma, T.; Kapustin, E. A.; Yin, S. X.; Liang, L.; Zhou, Z.; Niu, J.; Li, L.-H.; Wang, Y.; Su, J.; Li, J.; et al. Single-crystal x-ray diffraction structures of covalent organic frameworks. *Scienc* **2018**, *361*, 48–52.
- (19) (a) Colson, J. W.; Woll, A. R.; Mukherjee, A.; Levendorf, M. P.; Spittler, E. L.; Shields, V. B.; Spencer, M. G.; Park, J.; Dichtel, W. R. Oriented 2D Covalent Organic Framework Thin Films on Single-Layer Graphene. *Scienc* **2011**, *332*, 228–231. (b) Chandra, S.; Kundu, T.; Dey, K.; Addicoat, M.; Heine, T.; Banerjee, R. Interplaying Intrinsic and Extrinsic Proton Conductivities in Covalent Organic Frameworks. *Chem. Mater.* **2016**, *28*, 1489–1494. (c) Dogru, M.; Handloser, M.; Auras, F.; Kunz, T.; Medina, D.; Hartschuh, A.; Knochel, P.; Bein, T. A Photoconductive Thienothiophene-Based Covalent Organic Framework Showing Charge Transfer Towards Included Fullerene. *Angew. Chem., Int. Ed.* **2013**, *52*, 2920–2924.
- (20) (a) Sick, T.; Hufnagel, A. G.; Kampmann, J.; Kondofersky, I.; Calik, M.; Rotter, J. M.; Evans, A.; Döblinger, M.; Herbert, S.; Peters, K.; Böhm, D.; Knochel, P.; Medina, D. D.; Fattakhova-Rohlfing, D.; Bein, T. Oriented Films of Conjugated 2D Covalent Organic Frameworks as Photocathodes for Water Splitting. *J. Am. Chem. Soc.* **2018**, *140*, 2085–2092. (b) Vyas, V. S.; Haase, F.; Stegbauer, L.; Savasci, G.; Podjaski, F.; Ochsenfeld, C.; Lotsch, B. V. A Tunable Azine Covalent Organic Framework Platform for Visible Light-Induced Hydrogen Generation. *Nat. Commun.* **2015**, *6*, 8508.
- (21) Lohse, M. S.; Bein, T. Covalent Organic Frameworks: Structures, Synthesis, and Applications. *Adv. Funct. Mater.* **2018**, *28*, 1705553.
- (22) (a) Green, M. A.; Ho-Baillie, A.; Snaith, H. J. The Emergence of Perovskite Solar Cells. *Nat. Photonics* **2014**, *8*, 506–514. (b) Bu, T.; Liu, X.; Chen, R.; Liu, Z.; Li, K.; Li, W.; Peng, Y.; Ku, Z.; Huang, F.; Cheng, J.; Zhong, Y.-B. Organic/Inorganic Self-doping Controlled Crystallization and Electronic Properties of Mixed Perovskite Solar Cells. *J. Mater. Chem. A* **2018**, *6*, 6319–6326. (c) Wu, C.; Liu, Y.; Liu, H.; Duan, C.; Pan, Q.; Zhu, J.; Hu, F.; Ma, X.; Jiu, T.; Li, Z.; Zhao, Y. Highly Conjugated Three-Dimensional Covalent Organic Frameworks Based on Spirobifluorene for Perovskite Solar Cell Enhancement. *J. Am. Chem. Soc.* **2018**, *140*, 10016–10024.
- (23) (a) Stassen, I.; Styles, M.; Greci, G.; Gorp, H. V.; Vanderlinden, W.; Feyter, S. D.; Falcaro, P.; Vos, D. D.; Vereecken, P.; Ameloot, R. Chemical Vapour Deposition of Zeolitic Imidazolate Framework Thin Films. *Nat. Mater.* **2016**, *15*, 304–310. (b) Dong, R.; Zhang, T.; Feng, X. Interface-Assisted Synthesis of 2D Materials: Trend and Challenges. *Chem. Rev.* **2018**, *118*, 6189–6235.